

# Modeling and Simulation of Balanced Systems formed by Synchronous Generator-Infinite Bus in a Multi-Bond Graph Approach

GILBERTO GONZALEZ-AVALOS<sup>1</sup>, GERARDO AYALA-JAIMES<sup>2</sup>,  
TIZOC LOPEZ-L<sup>1</sup>, ALLEN A. CASTILLO BARRON<sup>2</sup>

<sup>1</sup>Faculty of Electrical Engineering, University of Michoacan,  
Avenida Francisco J. Múgica S/N Ciudad Universitaria C.P. 58030,  
Morelia,  
MÉXICO

<sup>2</sup>Faculty of Sciences of Engineering and Technology,  
Autonomous University of Baja California,  
Tijuana,  
MÉXICO

*Abstract:* - A basic electrical power system modeled in multi-bond graphs is proposed. This type of system comprises three phases from the applied synchronous generator, transmission line, and infinite bus, making it a multibody system, with multi-bond graphs being a versatile graphic methodology for this type of system. The mathematical modeling of the system is obtained from a proposed lemma. To show the behavior of the state variables of the system, simulation results are shown. This paper can be the basis for the modeling, analysis, and control of electrical power systems in a multi-bond graph approach.

*Key-Words:* - Multi-bond graph, bond graph, junction structure, synchronous generator, transmission line, infinite bus, Park transformation.

Received: May 21, 2024. Revised: October 24, 2024. Accepted: November 26, 2024. Published: December 31, 2024.

## 1 Introduction

The modeling of multibody systems has represented a challenge to have a model that allows analyzing its properties for its characterization, simulation, and control. Multibody systems are characterized by being formed by more than one dimension or coordinate, for example, robotic systems, aeronautical systems, and multi-phase electrical systems. The bond graph methodology has been used to model systems in graphic form that can be formed by several energy domains (electrical, mechanical, hydraulic, thermal) and their representation is in a unified form because the transfer of power is managed.

The first formal developments in the bond graph methodology can be found in [1] where bond graph modeling for physical systems is presented. Likewise, the analysis of linear systems in bond graphs is described. Another essential reference in bond graph modeling is in [2] where each element in the bond graph applied to linear and non-linear physical systems is explained in detail. The structural properties of a system modeled in a bond graph are presented in [3] here the properties of

observability and controllability for linear systems are introduced in a bond graph approach.

Multibody systems can be modeled with bond graphs, however, they result in extensive models that require in-depth knowledge of the system. Hence, multi-bond graphs appeared for the modeling of multibody systems and with the potential of bond graph analysis and synthesis tools. The essential references of multi-bond graphs are cited below: The elements in multi-bond graphs are described in [4]. Some relationships and definitions are found in [5]. A basic paper on the extension of the bond graph to a multi-bond graph is proposed in [6]. The modeling of mechanical systems in a robotics approach with multi-bond graphs is presented in [7]. Characteristics of the gyrators and junctions in multi-bond graphs are introduced in [8].

Some updated references in system modeling with multiband graphs are: The modeling of a prosthetic finger mechanism to control the trajectory and force in multi-bond graphs is proposed in [9]. Modeling the suspensions of a helicopter based on chains of kinematic joints is introduced in [10]. The steady-state response of alternating current circuits using multiband graphs is proposed in [11].

Linearization of a class of non-linear systems in a multi-bond graphs approach is proposed in [12]. The movements of translation and revolution under actuated joints of one-hand prostheses in a multiband graph are introduced in [13]. The modeling of electrical systems with multi-bond graphs is proposed in [14].

It is important to refer to some advances in electrical power systems: the analysis of synchronous machines and renewable generation converters for electromechanical oscillations is found in [15]. The control of synchronous capacitors and sources with inverters applied to small signal network models is proposed in [16]. A power system built by a synchronous generator, photovoltaic panels, and their connection to the infinite bus for small signal stability analysis is presented in [17].

In this paper, modeling with multi-bond graphs of a basic electrical energy generation system is proposed. This system is built by a synchronous generator, a transmission line connected to the infinite bus. Likewise, this three-phase system allows the direct application of multi-bond graphs, the mathematical model of the system based on a multiport junction structure in direct relation to traditional schemes is proposed through a lemma. In order to verify that the graphic model and the mathematical model obtained from the system are correct, simulation results are shown using 20-Sim software.

The contribution of this paper is to propose a multi-bond graph model of the electrical power system that has nonlinearities, being a compact model and that can be the basis for more complete systems of transmission line, loads and three phase electrical transformers that can be included in the system.

This approach has not been presented so far with multi-bond graphs and the proposed lemma determines a versatile way to obtain the state space of the system considering synchronous generator, transmission line and connection to the infinite bus. Section 2 describes the traditional scheme of a synchronous generator connected to an infinite bus through a serial transmission line. Section 3 describes the basic elements of multiband graph and the proposal of a lemma to obtain the mathematical model of the system. Section 4 presents the multi-bond graph of the electrical power system with the simulation results. Finally, the conclusions are given in Section 5.

## 2 Synchronous Generator Connected to an INFINITE BUS

Robust generation systems connect to transmission, distribution, and supply systems to loads through the infinite bus. A typical system of a synchronous generator connected to the infinite bus by means of a transmission line is shown in Figure 1, [18], [19], [20].

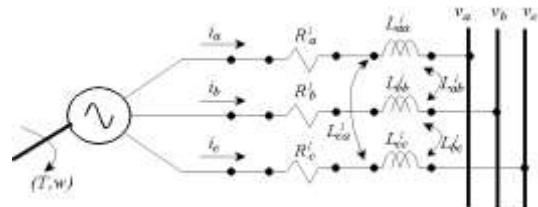


Fig. 1: Synchronous generator connected to an infinite bus

The three-phase voltage electrical power system in Figure 1 is defined by:

$$v_{abc}^G = R_{abc}^l i_{abc} + L_{abc}^l \frac{di_{abc}}{dt} + v_{abc}^\infty \quad (1)$$

where  $v_{abc}^G$  is the generator voltage;  $i_{abc}$  is the current supplied;  $v_{abc}^\infty$  is the bus voltage,  $R_{abc}^l$  and  $L_{abc}^l$  is the resistance and inductance of the transmission line, respectively.

A tool for simplifying the analysis in electrical power systems is the Park transformation that allows eliminating the time dependence in the equations. This transformation translates the coordinates (a,b,c) to an equivalent system in coordinates (d,q,0). This transformation for voltages, currents and flux links are defined by.

$$v_{dq0} = P v_{abc} \quad (2)$$

$$i_{dq0} = P i_{abc} \quad (3)$$

$$\lambda_{dq0} = P \lambda_{abc} \quad (4)$$

$$P = \sqrt{\frac{2}{3}} \begin{bmatrix} \cos \theta & \cos\left(\theta - \frac{2\pi}{3}\right) & \cos\left(\theta + \frac{2\pi}{3}\right) \\ \sin \theta & \sin\left(\theta - \frac{2\pi}{3}\right) & \sin\left(\theta + \frac{2\pi}{3}\right) \\ \frac{1}{\sqrt{2}} & \frac{1}{\sqrt{2}} & \frac{1}{\sqrt{2}} \end{bmatrix} \quad (5)$$

with

$$\theta = \omega t + \delta + \frac{\pi}{2} \quad (6)$$

being  $\omega$  is the angular frequency in rad/s and  $\delta$  is the synchronous torque angle.

Applying the Park transformation to (1)

$$v_{dq0}^G = R_{dq0}^l i_{dq0} + L_{dq0}^l \left( \frac{di_{dq0}}{dt} - \frac{dP\%}{dt} P^{-1} i_{dq0} \right) + v_{dq0}^\infty \quad (7)$$

where

$$R_{dq0}^l = PR_{abc}^l P^{-1} \quad (8)$$

$$L_{dq0}^l = PL_{abc}^l P^{-1} \quad (9)$$

and

$$\frac{dP}{dt} P^{-1} = X(\omega) = \begin{bmatrix} 0 & -\omega & 0 \\ \omega & 0 & 0 \\ 0 & 0 & 0 \end{bmatrix} \quad (10)$$

(7) with (10) reduces to

$$v_{dq0}^G = R_{dq0}^l i_{dq0} + L_{dq0}^l \frac{di_{dq0}}{dt} - L_{dq0}^l X(\omega) i_{dq0} + v_{dq0}^\infty \quad (11)$$

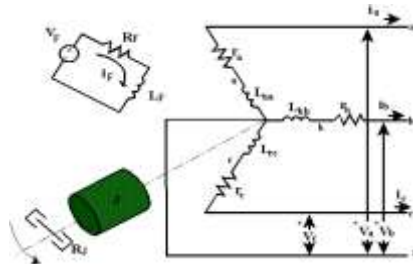


Fig. 2: Synchronous generator

Now, the model of the synchronous generator in coordinates (d,q,0) is shown in Figure 2 and its mathematical model is described by [18], [19], [20].

$$\begin{bmatrix} L_{dq0}^G & M^T & 0 \\ M & L_F & 0 \\ 0 & 0 & J \end{bmatrix} \begin{bmatrix} \frac{di_{dq0}}{dt} \\ \frac{di_F}{dt} \\ \frac{dw}{dt} \end{bmatrix} = \begin{bmatrix} -R_{dq0}^G & 0 & -(\lambda^G)^T \\ 0 & -R_F & 0 \\ \lambda^G & 0 & -R_J \end{bmatrix} \begin{bmatrix} i_{dq0} \\ i_F \\ w \end{bmatrix} + \begin{bmatrix} -v_{dq0}^G \\ V_F \\ T_m \end{bmatrix} \quad (12)$$

where  $v_{dq0}^G$  are the voltages at the generator terminals;  $i_{dq0}$  the current generated,  $i_F$  and  $R_F$  the current and resistance in the field winding, respectively;  $\omega$  the velocity;  $T_m$  the input mechanical torque;  $L_F$  and  $R_F$  the inductance and resistance of the field winding, respectively;  $J$  and  $R_J$  the inertia and friction of the machine, respectively;  $L_{dq0}^G$  and  $R_{dq0}^G$  the inductance and resistance of the armature winding, respectively;

$M = [M_{dF} \ 0 \ 0]$  the mutual inductance of the armature and field windings;  $\lambda^G = [\lambda_q \ -\lambda_d \ 0]$  machine flow links.

### 3 Systems Modelling in Multi-Bond Graphs

Multibody systems are characterized by having several signals that depend on each other, so modeling these systems with individual signals results in extensive and complicated representations for analysis, synthesis and simulation.

Multi-bond graphs represent a graphical modeling tool for multibody systems that has the versatility of the analysis of bond graphs that are well known. When two multibody system signals are connected, there is always power transfer  $\underline{P}(t)$  because there is a unified frame of reference in multiband graph generalized power variables called effort vector  $\underline{e}(t)$  and flow vector  $\underline{f}(t)$  are used in multi-bond graph, these variables determine the power vector:

$$\underline{P}(t) = \underline{e}^T(t) \cdot \underline{f}(t) \quad (13)$$

where

$$\underline{e}(t) = \begin{bmatrix} e^a(t) \\ e^b(t) \\ e^c(t) \end{bmatrix}; \quad \underline{f}(t) = \begin{bmatrix} f^a(t) \\ f^b(t) \\ f^c(t) \end{bmatrix}$$

In the different energy domains, the generalized variables are indicated in Table 1.

Table. 1 Power variables

System	Effort [ $e(t)$ ]	Flow [ $f(t)$ ]
Electrical	Voltage [ $v(t)$ ]	Current [ $i(t)$ ]
Mechanical	Force [ $F(t)$ ] Torque [ $\tau(t)$ ]	Velocity [ $v(t)$ ] Ang. velocity [ $\omega(t)$ ]
Hydraulic	Pressure [ $P(t)$ ]	Volume flow rate [ $Q(t)$ ]

The energy variables in multi-bond graphs are: momentum  $\underline{p}(t)$  and displacement  $\underline{q}(t)$ , and are related to the power variables by:

$$\underline{p}(t) = \int \underline{e}(t) dt \quad (14)$$

$$\underline{q}(t) = \int \underline{f}(t) dt \quad (15)$$

The basic element of multi-bond graph that determines the connection of components is the multi bond shown in Figure 3. Likewise, the application of causality is indicated, which is drawn by a vertical line that indicates the direction of the effort and the flow in the opposite direction.

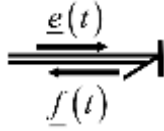


Fig. 3: Causal multi-bond

Power supply elements are  $(\underline{MS}_e(t), \underline{MS}_e(t))$  multiport effort source and multiport flow source, respectively, shown in Figure 4.

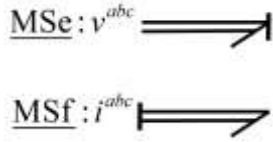


Fig. 4: Multiport sources

The dissipative elements are shown in Figure 5 whose constitutive functions are a function of the causality given by:

$$\underline{e}(t) = \Phi_{R_1}[\underline{f}(t)] \quad (16)$$

$$\underline{f}(t) = \Phi_{R_2}[\underline{e}(t)] \quad (17)$$

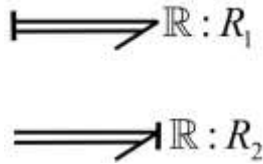


Fig. 5: Multiport resistors

The storage elements are inertias and capacitances. Figure 6 illustrates inertia in integral causality assignment where the constitutive relationship is:

$$\underline{f}(t) = \Phi_I^{-1}\left[\int \underline{e}(t) dt\right] = \Phi_I^{-1}[\underline{p}(t)] \quad (18)$$

for a linear relationship:

$$\underline{f}(t) = \mathbf{L}^{-1} \int \underline{e}(t) dt = \mathbf{L}^{-1} \underline{p}(t) \quad (19)$$



Fig. 6: Multiport inertia in integral causality

If this element is in derivative causality assignment, the constitutive relationship is:

$$\underline{e}(t) = \frac{d\Phi_I[\underline{f}(t)]}{dt} \quad (20)$$

shown in Figure 7.

The other storage element in integral causality is the capacitor illustrated in Figure 8.



Fig. 7: Multiport inertia in derivative causality



Fig. 8: Multiport capacitor in integral causality with the constitutive relationship:

$$\underline{e}(t) = \Phi_C^{-1}\left[\int \underline{f}(t) dt\right] = \Phi_C^{-1}[\underline{q}(t)] \quad (21)$$

if it is linear:

$$\underline{e}(t) = \mathbf{C}^{-1} \int \underline{f}(t) dt = \mathbf{C}^{-1} \underline{q}(t) \quad (22)$$

In case it has derivative causality, thus element is shown in Figure 9.



Fig. 9: Multiport capacitor in derivative causality

with the constitutive relationship:

$$\underline{f}(t) = \frac{d\Phi_C[\underline{e}(t)]}{dt} \quad (23)$$

The power transfer elements from one port to another are defined by multiport transformers and gyrators shown in Figure 10.

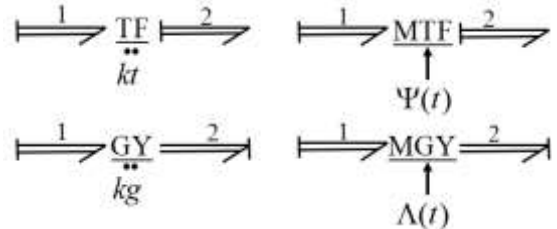


Fig. 10: Multiport transformers and gyrators

The multiport transformer ( $\underline{TF}$ ) has the constitutive relationship:

$$\begin{bmatrix} \underline{e}_1 \\ \underline{f}_1 \end{bmatrix} = \begin{bmatrix} K_t^{-1} & 0 \\ 0 & K_t \end{bmatrix} \begin{bmatrix} \underline{e}_2 \\ \underline{f}_2 \end{bmatrix} \quad (24)$$

If it is a multiport modulated transformer ( $\underline{MTF}$ ) then  $K_t = \Psi(t)$  that is the modulated signal.

The constitutive relation of the multiport gyrator ( $\underline{GY}$ ) is:

$$\begin{bmatrix} \underline{e}_1 \\ \underline{f}_1 \end{bmatrix} = \begin{bmatrix} 0 & K_g \\ K_g^{-1} & 0 \end{bmatrix} \begin{bmatrix} \underline{e}_2 \\ \underline{f}_2 \end{bmatrix} \quad (25)$$

If it is a modulated multiport gyrator ( $\underline{MGY}$ ) then  $K_g = \Lambda(t)$  that is the modulated signal.

The elements that allow the connection of the different multiport elements are the connections shown in Figure 11.

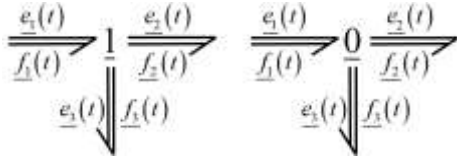


Fig. 11: Multiport junctions

The effort and flow relationships for multiport junction (1) are defined by:

$$\underline{e}_1 = \underline{e}_2 + \underline{e}_3; \underline{f}_1 = \underline{f}_2 = \underline{f}_3 \quad (26)$$

and for the multiport junction (0) they are:

$$\underline{e}_1 = \underline{e}_2 = \underline{e}_3; \underline{f}_1 = \underline{f}_2 + \underline{f}_3 \quad (27)$$

The different multiport elements of a system modeled by multi-bond graphs can be organized by fields to obtain the mathematical model of the system, which is illustrated in Figure 12.

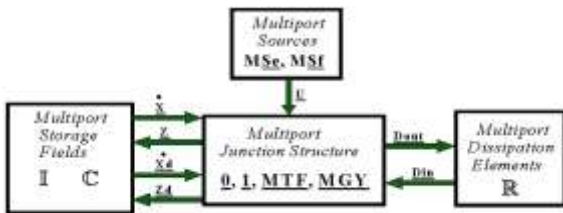


Fig. 12: Junction structure of a multi-bond graph

The block diagram in Figure 12 indicates the following fields:

- The multiport sources with input  $\underline{u}(t) \in \mathfrak{R}^p$ .
- The multiport states  $\underline{x}(t) \in \mathfrak{R}^n$  which are the elements (C, I) in integral causality and the multiport co-energy vector  $\underline{z}(t) \in \mathfrak{R}^n$ .
- The multiport states  $\underline{xd}(t) \in \mathfrak{R}^m$  that are states linearly dependent on  $\underline{x}(t)$  and with the multiport coenergy vector  $\underline{zd}(t) \in \mathfrak{R}^m$ .
- Multiport dissipation elements (R) are related to the junction structure by  $\underline{D}_{in} \in \mathfrak{R}^r$  and  $\underline{D}_{out} \in \mathfrak{R}^r$ .
- The multiport junction structure is formed by (1, 0) and by multiport transformers and gyrators (MTF, MGY).

The different fields and key vectors that determine the mathematical model of a multi-bond graph for an electrical system are described in the following lemma.

### Lemma

Consider a multi-body system modeled by a multi-bond Graph with predefined integral causality assignment according to Figure 12 with a multiport junction structure defined by

$$\begin{bmatrix} \dot{\underline{x}} \\ \underline{D}_{in} \\ \underline{z}_d \end{bmatrix} = \begin{bmatrix} \mathbf{S}_{11} & \mathbf{S}_{12} & \mathbf{S}_{13} & \mathbf{S}_{14} \\ \mathbf{S}_{21} & \mathbf{S}_{22} & \mathbf{S}_{23} & \mathbf{0} \\ \mathbf{S}_{31} & \mathbf{0} & \mathbf{0} & \mathbf{0} \end{bmatrix} \begin{bmatrix} \underline{z} \\ \underline{D}_{out} \\ \underline{u} \\ \dot{\underline{x}}_d \end{bmatrix} \quad (28)$$

with constitutive relations of the multiport fields given by:

$$\underline{z} = \mathbf{F}\underline{x} \quad (29)$$

$$\underline{z}_d = \mathbf{F}_d \underline{x}_d \quad (30)$$

$$\underline{D}_{out} = \mathbf{L}\underline{D}_{in} \quad (31)$$

then a state space model of the system is described by:

$$\mathbf{E}(\underline{x}) \dot{\underline{z}} = \mathbf{A}(\underline{x}) \underline{z} + \mathbf{B}(\underline{x}) \underline{u} \quad (32)$$

where

$$\mathbf{E}(\underline{x}) = \mathbf{F}^{-1} - \mathbf{S}_{13} \mathbf{F}_d^{-1} \mathbf{S}_{31} \quad (33)$$

$$\mathbf{A}(\underline{x}) = \mathbf{S}_{11} + \mathbf{S}_{12} \mathbf{M} \mathbf{S}_{21} \quad (34)$$

$$\mathbf{B}(\underline{x}) = \mathbf{S}_{13} + \mathbf{S}_{12} \mathbf{M} \mathbf{S}_{23} \quad (35)$$

with

$$\mathbf{M} = \mathbf{L}(\mathbf{I} - \mathbf{S}_{22} \mathbf{L})^{-1} \quad (36)$$

Proof. From the second line of (28) with (31)

$$\underline{D}_{in} = (\mathbf{I} - \mathbf{S}_{22} \mathbf{L})^{-1} (\mathbf{S}_{21} \underline{z} + \mathbf{S}_{23} \underline{u}) \quad (37)$$

from the third line of (28) with (29) and (30), the relationship of linearly independent and dependent elements is:

$$\underline{x}_d = \mathbf{F}_d^{-1} \mathbf{S}_{31} \underline{x} \quad (38)$$

differentiating with respect to time (38) and replacing in the first line of (28) with (37) and (29)

$$(\mathbf{F}^{-1} - \mathbf{S}_{13} \mathbf{F}_d^{-1} \mathbf{S}_{31}) \dot{\underline{z}} = (\mathbf{S}_{11} + \mathbf{S}_{12} \mathbf{M} \mathbf{S}_{21}) \underline{z} + (\mathbf{S}_{13} + \mathbf{S}_{12} \mathbf{M} \mathbf{S}_{23}) \underline{u} \quad (39)$$

substituting (33), (34) and (35) into (39), the state space given in (32) is proven.

The proposed lemma allows obtaining the mathematical model of a system modeled in multi-bond graph, having the advantage of determining the state space in a structured way.

## 4 Systems Modeling in Multi-Bond Graphs

The multi-bond graph model of the system formed by a synchronous generator connected to the infinite bus through a transmission line is shown in Figure 13.

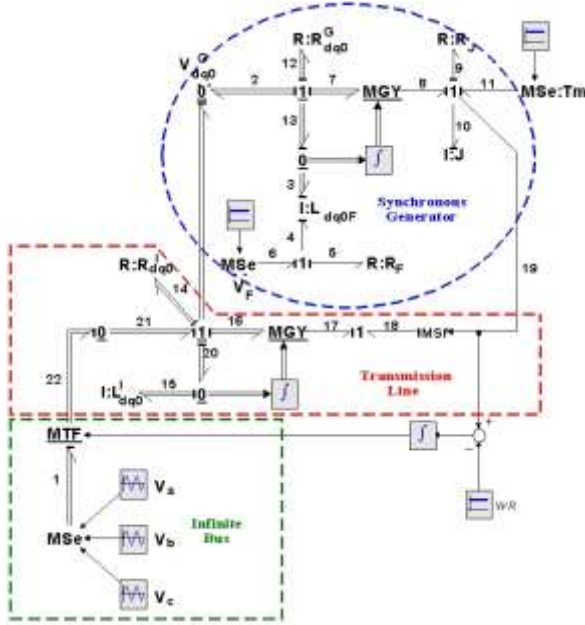


Fig. 13: Multi-bond graph system

In Figure 13 the synchronous generator is inside the blue dotted area, in the armature winding in coordinates  $(d,q,0)$  we have the multiport resistance  $\mathbb{R}: R_{dq0}^G$  and the multiport field inductance  $I: L_{dq0}^G$  magnetically connected to the field winding with resistance  $R: R_F$  and the DC voltage in this winding  $MSe: V_F$ ; the mechanical section of the generator consists of the inertia  $I: J$ , the air friction  $R: R_J$  and the input torque of the prime-motor  $MSe: T_m$  which is related to the armature winding by the multiport gyrator modulated by the flux links of the machine. The transmission line within the red dotted area is modeled by the multiport resistor  $\mathbb{R}: R_{dq0}^l$  in series with the multi-port inductance  $I: L_{dq0}^l$  and connected to the generator by the multiport gyrator modulated by the line flux links and machine speed.

The infinite bus inside the green dotted area is the three-phase voltage  $MSe: V_{abc}^\infty$ ,

The key vectors of the system are:

$$\underline{x} = \begin{bmatrix} p_3 \\ p_4 \\ p_{10} \end{bmatrix}; \quad \dot{\underline{x}} = \begin{bmatrix} e_3 \\ e_4 \\ e_{10} \end{bmatrix}; \quad \underline{z} = \begin{bmatrix} f_3 \\ f_4 \\ f_{10} \end{bmatrix}; \quad \underline{D}_{in} = \begin{bmatrix} f_{12} \\ f_5 \\ f_9 \\ f_{14} \end{bmatrix}; \quad \underline{D}_{out} = \begin{bmatrix} e_{12} \\ e_5 \\ e_9 \\ e_{14} \end{bmatrix}$$

$$\underline{u} = \begin{bmatrix} e_1 \\ e_6 \\ e_{11} \end{bmatrix}; \quad \underline{x}_d = p_{15}; \quad \dot{\underline{x}}_d = e_{15}; \quad \underline{z}_d = f_{15}$$

with the constitutive relations

$$\mathbf{F}^{-1} = \begin{bmatrix} L_{dq0}^G & M^T & 0 \\ M & L_F & 0 \\ 0 & 0 & J \end{bmatrix} \quad (40)$$

$$\mathbf{L} = \text{diag} \{ R_{dq0}^G, R_F, R_J, R_{dq0}^l \} \quad (41)$$

$$F_d = L_{dq0}^l \quad (42)$$

where

$$M = [M_{dF} \quad 0 \quad 0]; \quad L_{dq0}^G = \text{diag} \{ L_d^G, L_q^G, L_0^G \}$$

$$L_{dq0}^l = \text{diag} \{ L_d^l, L_q^l, L_0^l \}; \quad R_{dq0}^G = \text{diag} \{ R_d^G, R_q^G, R_0^G \}$$

$$R_{dq0}^l = \text{diag} \{ R_d^l, R_q^l, R_0^l \}$$

whose multi-port junction structure matrix is described by:

$$\begin{bmatrix} e_3 \\ e_4 \\ e_{10} \\ f_{12} \\ f_5 \\ f_9 \\ f_{14} \\ f_{15} \end{bmatrix} = \begin{bmatrix} 0 & 0 & \lambda^l - \lambda^G & -\mathbf{I} & 0 & 0 & \mathbf{I} & -\mathbf{I} & 0 & 0 & \mathbf{I} \\ 0 & 0 & 0 & 0 & -1 & 0 & 0 & 0 & 1 & 0 & 0 \\ (\lambda^G)^T & 0 & 0 & 0 & 0 & -1 & 0 & 0 & 0 & 1 & 0 \\ \mathbf{I} & 0 & 0 & 0 & 0 & 0 & 0 & 0 & 0 & 0 & 0 \\ 0 & 1 & 0 & 0 & 0 & 0 & 0 & 0 & 0 & 0 & 0 \\ 0 & 0 & 1 & 0 & 0 & 0 & 0 & 0 & 0 & 0 & 0 \\ -\mathbf{I} & 0 & 0 & 0 & 0 & 0 & 0 & 0 & 0 & 0 & 0 \\ -\mathbf{I} & 0 & 0 & 0 & 0 & 0 & 0 & 0 & 0 & 0 & 0\% \end{bmatrix} \begin{bmatrix} f_3 \\ f_4 \\ f_{10} \\ e_{12} \\ e_5 \\ e_9 \\ e_{14} \\ e_1 \\ e_6 \\ e_{11} \\ e_{15} \end{bmatrix} \quad (43)$$

From (33), (40), (42) and (43) the inductance matrix is given by:

$$E(x) = \begin{bmatrix} L_{dq0}^G + L_{dq0}^l & M^T & 0 \\ M & L_F & 0 \\ 0 & 0 & J \end{bmatrix}$$

From (34), (41), and (43) the nonlinear state matrix is:

$$A(x) = \begin{bmatrix} -R_{dq0}^G - R_{dq0}^l & 0 & \lambda^l - \lambda^G \\ 0 & -R_F & 0 \\ (\lambda^G)^T & 0 & -R_J \end{bmatrix}$$

and from (35) and (43) the input matrix is:

$$B(x) = \begin{bmatrix} -I & 0 & 0 \\ 0 & 1 & 0 \\ 0 & 0 & 1 \end{bmatrix}$$

The behavior of the system state variables is achieved from the simulation of the multi-bond graph in Figure 13, which is carried out in 20-Sim software. The numerical parameters of the system are given by  $v_a=200\sin(\omega t)V$ ,  $v_b=200\sin(\omega t-120)V$ ,  $v_c=200\sin(\omega t-120)V$ ,  $V_F=30V$ ,  $T_m=100Nm$ ,  $R_J=1Nms$ ,  $R_F=0.95\Omega$ ,  $R_{dq0}^G = \text{diag}\{0.5, 0.5, 0.5\}\Omega$ ,  $R_{dq0}^l = \{0.01, 0.01, 0.01\}\Omega$ ,  $J=2.37Nms^2$ ,  $L_F=1.65H$ ,  $L_{dq0}^G = \text{diag}\{0.5, 0.5, 0.5\}H$ ,  $L_{dq0}^l = \text{diag}\{0.01, 0.01, 0.01\}H$ ,  $M_{dF}=1.55H$ ,  $F=60Hz$ .

Figure 14 illustrates the performance of the currents supplied from the generator to the infinite bus  $idq0$ , because the system is balanced and stable, the currents stabilize at  $i_d = -27.4497A$ ,  $i_q = 0.087A$ ,  $i_0 = 0$ ,  $i_F = 31.5798A$ ,  $\omega = 95.80rad/s$ .

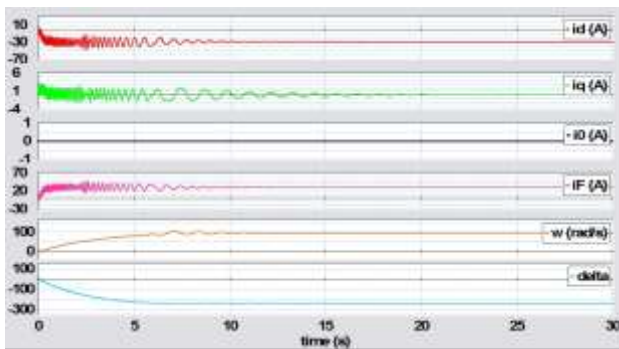


Fig. 14: Behavior of generator variables

The currents supplied by the generator in the time domain, that is, in coordinates (a, b, c),  $i_{abc}$  are shown in Figure 15, observing that the system is stable. Likewise, in Figure 16 shows the currents  $i_{abc}$  in a short time range of 24.95s to 25.2s this graph illustrates that there is the phase shift of a balanced system of  $120^\circ$ .

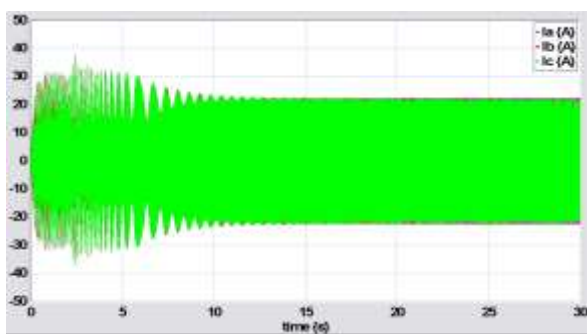


Fig. 15: Currents supplied to the system

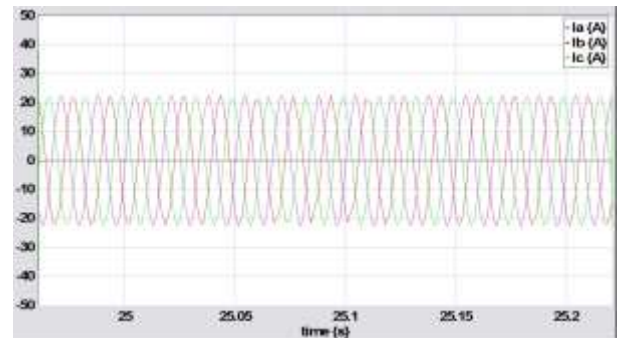


Fig. 16: iabc currents in a short period of time

## 5 Conclusion

The multi-bond graph methodology in the modeling of a synchronous generator, transmission line and its connection to an infinite bus has been applied. Because these systems are made up of three phases, multi-bond graphs represent an effective alternative to obtain compact models. A lemma has been proposed to determine the mathematical model from its multi-bond graph. Simulation results are shown to verify the behavior of the system variables.

### References:

- [1] D. C. Karnopp, D. L. Margolis, R. C. Rosenberg, *System dynamics modeling and simulation of mechatronic systems*, USA, Wiley Interscience, 2000.
- [2] F. T. Brown, *Engineering system dynamics*, USA, Marcel Dekker, Inc. 2001.
- [3] C. Sueur and G. Dauphin-Tanguy, Bond graph approach for structural analysis of MIMO linear system, *Journal of the Franklin Institute*, Vol. 328, No. 1, pp. 55-70, 1991.
- [4] P. C. Breedveld, Multibody graph elements in physical systems theory, *Journal of the Franklin Institute*, Vol. 319, No. 1/2, pp. 1-36, 1985.
- [5] W. Borutzky, G. Dauphin-Tanguy, J. U. Thoma, Advances in bond graph modelling: Theory, software, applications, *Math. Comput. Simul.*, Vol. 39, No. 5-6, pp. 465-475, 1995.
- [6] S. Behzadipour, A. Khajepour, Causality in vector bond graphs and its application to modeling of multi-body dynamic systems, *Simul. Modell. Pract. Theory*, Vo. 14, No. 3, pp. 279-295, 2006.
- [7] M. J. L. Tiernego, A. M. Bos, Modelling the dynamics and kinematics of mechanical systems with multibond graphs, *Journal of the Franklin Institute*, Vol. 319, No. 1/2, pp. 37-50, 1985.

- [8] P. C. Breeveld, Essential gyrators and equivalence rules for 3-port junction structures, *Journal of the Franklin Institute*, Vol. 318, No. 2 pp. 77-89, 1984.
- [9] N. Mishra, A Vaz, Development of trajectory and force controllers for 3-joint string- tube actuated finger prosthesis based on bond graph modeling, *Mechanism and Machine Theory*, Vol. 146, 103719, April 2020.
- [10] B. Boundon, F. Malburet, J. C. Carmona, Design Methodology of a Complex CKC Mechanical Joint with an Energetic Representation Tool "Multibond Graph": Application to the Helicopter, *Multibody Dynamics*, 332 (1), *Springer International Publishing*, pp. 387-429, 2017.
- [11] Nunez, P. C. Breedveld, and P.B. T. Weustink, Steady-State power flow analysis of electrical power systems modelled by 2-dimensional multibond graphs, *Proceeding of the International Conference on Integrated Modeling and Analysis in Applied Control and Automation*, pp. 39-47, Italy, September 21-23, 2015.
- [12] G. Gonzalez, G. Ayala, N. Barrera and A. Padilla, Linearization of a Class of Nonlinear Systems Modelled by Multibond Graphs, *Mathematical and Computer Modelling of Dynamical Systems*, Vol. 25, No. 3, pp. 284-332, 2019.
- [13] N. Mishra, A. Vaz, Bond graph modeling of a 3-joint String-Tube Actuated finger prosthesis, *Mechanism and Machine Theory*, Vo. 117, pp. 1-20, 2017.
- [14] G. Gonzalez, N. Barrera, G. Ayala, A Padilla, Modeling and Simulation in Multibond Graphs Applied to Three-Phase Electrical Systems, *Appl. Sci.*, 2023, 13 (10), 5880.
- [15] L. Benedetti, P. N. Papadopoulos, A. E. Alvarez, Small Signal Interactions Involving a Synchronous Machine and a Grid Forming Converter, In *Proceedings of the 2021 IEEE Madrid Power Tech.*, Madrid, Spain, 28-June-2, July 2021, <https://doi.org/10.1109/PowerTech46648.2021.9494923>.
- [16] L. Ding, X. Liu, J. Tan, Small-Signal Stability Analysis of the Power System Based on Active Support of Renewable Energy VSCs. *Front Energy Res.*, 2022, 10, 907790.
- [17] S. Izumi, Y. Karakawa, X Xin, Analysis of small-signal stability of power systems with photovoltaic generators, *Electr. Eng.*, Vol. 101, pp. 321-331, 2019.
- [18] J. R. Kundur, *Power System Stability and Control*, Mc. Graw-Hill, New York, NY, USA, 1994.
- [19] P. M. Anderson, *Power System Control and Stability*, The Iowa State University Press, Ames, IA, USA, 1977.
- [20] P. C. Krause, O. Wasynczuk, S. D. Sudhoff, Analysis of Electrical Machinery and Drive Systems, *IEEE Press, Wiley- Interscience*, 2002.

#### **Contribution of Individual Authors to the Creation of a Scientific Article (Ghostwriting Policy)**

The authors equally contributed in the present research, at all stages from the formulation of the problem to the final findings and solution.

#### **Sources of Funding for Research Presented in a Scientific Article or Scientific Article Itself**

No funding was received for conducting this study.

#### **Conflict of Interest**

The authors have no conflicts of interest to declare.

#### **Creative Commons Attribution License 4.0 (Attribution 4.0 International, CC BY 4.0)**

This article is published under the terms of the Creative Commons Attribution License 4.0

[https://creativecommons.org/licenses/by/4.0/deed.en\\_US](https://creativecommons.org/licenses/by/4.0/deed.en_US)